Article:
Shi, H., Worden, K. and Cross, E.J. (2019) A cointegration approach for heteroscedastic data based on a time series decomposition: An application to structural health monitoring. Mechanical Systems and Signal Processing, 120. pp. 16-31. ISSN: 0888-3270

https://doi.org/10.1016/j.ymssp.2018.09.036

Mechanical Systems and Signal Processing 120 (2019) 16–31

Contents lists available at ScienceDirect

Mechanical Systems and Signal Processing

journal homepage: www.elsevier.com/locate/ymssp

A cointegration approach for heteroscedastic data based on a time series decomposition: An application to structural health monitoring

Haichen Shi, Keith Worden, Elizabeth J. Cross *

Dynamics Research Group, Department of Mechanical Engineering, University of Sheffield, Mappin Street, Sheffield S1 3JD, United Kingdom

ARTICLE INFO

Article history:
Received 10 April 2018
Received in revised form 20 September 2018
Accepted 28 September 2018

Keywords:
Structural health monitoring
Environmental and operational variation
Cointegration
Heteroscedasticity
TBATS model
Time series

ABSTRACT

Heteroscedasticity, or time-dependent variance, is often observed in long-term monitoring data in the context of SHM, where it is normally induced by the seasonal variations of the ambient environment. In the effort to project out the environmental and operational variations, cointegration, a method originating in econometrics, has been successfully employed in various SHM studies. This paper will explore a possible enhanced approach to cointegration, to make it applicable to heteroscedastic data. The fact that the variance of heteroscedastic data is constantly changing has a significant negative impact on conventional damage detection algorithms, making it difficult to calculate accurate confidence intervals. Thus, in the current paper, an exponential smoothing method is presented to explore and deal with the complex seasonal patterns observed in SHM time series. More specifically, in this framework, a seasonally-corrupted time series can be decomposed into three components, namely, level, seasonal and residual terms. Subsequently, the series purged of seasonality will be fed into a cointegration analysis, in order to produce a more stationary residual series (damage indicator series). Two case studies, including a synthetic case and a real world SHM dataset, are demonstrated with results and discussions.

1. Introduction

Structural Health Monitoring (SHM) is increasingly crucial for the maintenance of important infrastructure; research work in this area has seen a dramatic boost in the last decade. One of the major obstacles holding back the transition of SHM from the laboratory and theoretical research to real-world engineering practice is the confounding influence of the environmental and operational variations (EOVs). As elaborated in [1], "without intelligent feature extraction, the more sensitive a measurement is to damage, the more sensitive it is to changing operational and environmental conditions". Before building a damage detection algorithm, the normal baseline state of the underlying structure firsts needs to be accurately identified. Thermal conditions, for example, may account for 5% to 10% of the variations of the modal properties of bridges [2,3]; daily traffic loading variations may cause up to a 5.4% shift in the first natural frequency of a plate-girder bridge [4]. An introductory survey of EOV effects on SHM can be found in [5]; readers can also find some of the latest developments in EOV effects in [6–9].

In recent work of the last two authors here, cointegration, a method originating in econometrics, has been successfully adapted to effectively remove the effects of EOVs in SHM data [10]. *Cointegration* is a property of nonstationary time series;

* Corresponding author.
E-mail address: e.j.cross@sheffield.ac.uk (E.J. Cross).

https://doi.org/10.1016/j.ymssp.2018.09.036
0888-3270/

two nonstationary time series can be said to be cointegrated if some linear combination of them forms a stationary series. Perhaps one of the most successful applications of cointegration is in the pairs trading strategy to financial time series, where two highly-correlated time series are paired to form a stationary cointegrated residual, purged of the variations caused by market volatility [11]. Analogously, in the context of SHM, the EOVs may be regarded as some set of stochastic common trends affecting the dynamic behaviour of the structure simultaneously. By building the cointegration relationship among the measurements of the structure, one can find a stationary cointegrated residual with the EOVs eliminated, which can be used as an efficient damage indicator. After the first introduction of cointegration to SHM [10], a number of exploratory studies have been carried out to further enhance the applicability of the cointegration method. In an effort to analyse the nonstationarity of a time series, Worden et al. [12] utilise discrete wavelet analysis as a means of characterising the time scale on which nonstationarity manifests itself. By finding the 'most nonstationary' time scale, one may possibly enhance the damage sensitivity of the cointegration method. The authors of this paper also attempted to use Gaussian Processes to build a nonlinear cointegration relationship, so as to model the distinct behaviour of bridges during summer and winter time [13]. Zolna et al. presented a nonlinear cointegration approach using a scaling transformation that can produce a variance-stationary residual series [14]. A more recent review paper on time series methods was presented by Worden et al. [15]; they reviewed the latest developments of time series algorithms in the field and imposed two open problems regarding cointegration analysis; namely heteroscedasticity and nonlinearity. This paper will attempt to address the first of these issues.

With the rapid advancement of sensing technology, the availability and accessibility of all kinds of data from structures has been greatly improved. As the duration of recorded data grows, seasonal effects become inevitably important, especially for long-term monitoring. Meteorological variations and human activities might couple with the behaviour of the structures, making the modelling of underlying states of the structure extremely difficult. More specifically, the seasonal effects may produce input-dependent noise in the measurements of the structure, or heteroscedastic noise, as in the statistical literature. As is well known, many statistical and machine learning estimation methods are based on ordinary least squares (OLS) or maximum likelihood; thus heteroscedastic noise may bias the estimation of the model, causing misleading judgements of the health state of the structure. Therefore, this study seeks to further strengthen the practice of the cointegration method; a well-established method from the time series literature, called the TBATS (**T**rigonometric, **B**ox-Cox transform, **A**RMA errors, **T**rend, and **S**easonal components) model [16], is explored to deal with seasonal effects in SHM data. After suppressing the heteroscedasticity in the series, cointegration analysis is performed to build a damage sensitive residual series.

This paper begins with a motivating example, followed by brief theoretical introductions to the exponential smoothing method and the TBATS model, it will then go on to an introduction and a brief review of the cointegration method. A synthetic case study will be presented in the fifth part to illustrate the proposed method. Another case study, of the National Physical Laboratory (NPL) Bridge with the proposed method, is presented in the same section, the last part includes summary and some discussions.

2. A motivating example

Nowadays, many long-term SHM studies have continuously collected years worth of sensor data from structures. When time span and resolution of available data are comprehensive enough, accounting for seasonality or periodicity becomes crucial for data modelling.

Consider the National Physical Laboratory (NPL) Bridge, for example [17]. The NPL Bridge was monitored for an extensive time span meaning that the data capture a wide range of behaviours induced by environmental variations. The monitoring campaign also introduced several kinds of damage scenarios to the bridge. However, observing time series of measured tilt data, as shown in Fig. 1, no immediate damage information is available as it is overwhelmed by the environmental variations. These time series are clearly nonstationary, both in mean and variance, with unfortunately few methods being valid for such time series. Worden et al. [18] attempted to model the tilt sensor data using the linear cointegration method (theories of which will be reviewed shortly).

Cointegration was applied to the eight tilt sensor time series, in order to form a stationary residual for damage detection purposes. As demonstrated in Fig. 2, the vertical black line shows the end of the training samples for cointegration, which accounted for a full year of environmental variations. The residual series clearly possesses time-varying variance, the underlying seasonality has severely undermined the effectiveness of the algorithm. With the help of the Statistical Process Control (SPC) chart, the "X-bar chart" in this case [19], the situation can be somewhat alleviated. The measurements of the tilt sensor were hourly-based, every 24 measurements were averaged to obtain a daily representative sample, the resulting residual series is shown in Fig. 3, the horizontal dashed lines indicate $\pm 3\sigma$ (standard deviation) control limits, the vertical blue line marks where the first damage scenario was implemented. Despite the nonstationarity in the residual variance, the algorithm clearly retains the power of damage detection, such that after the damage introduction, the mean of the residual gradually goes beyond the control limits.

In terms of seasonality/periodicity in the NPL Bridge data, the daily cycle is an apparent one (usually synchronised with the daily cycle of temperature). Another important observation is that as time approaches the middle of a year, the amplitude of the daily cycle gets bigger as well, it will then shrink towards the end of a year. This might be caused by the fact that the tilt sensors are generally sensitive to temperature variations, such that their associated measuring errors

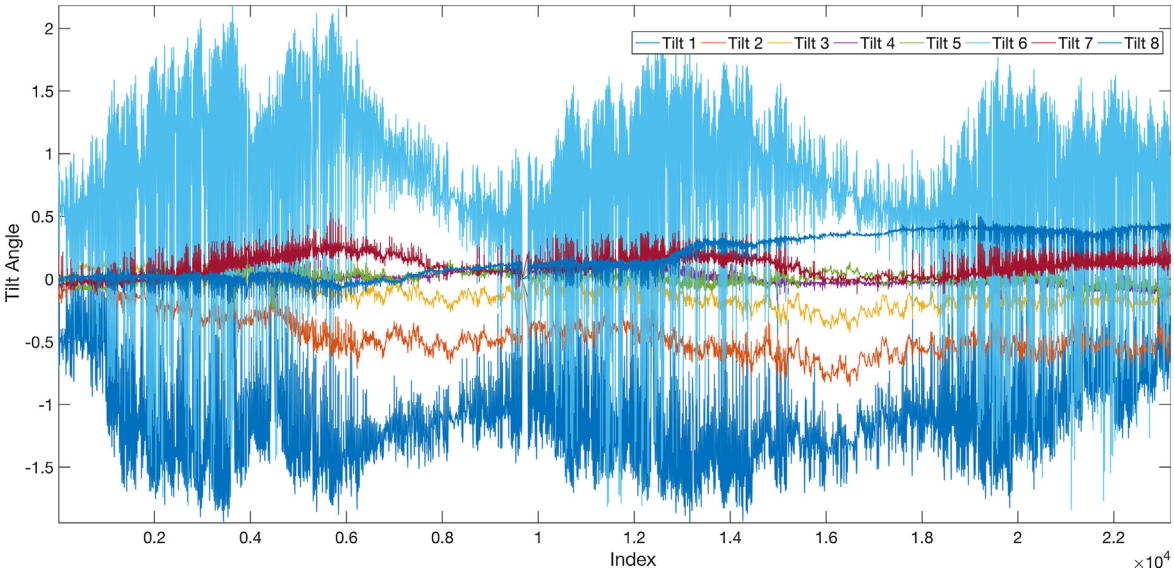

Fig. 1. Data collected from all 8 tilt sensors installed on the NPL Bridge.

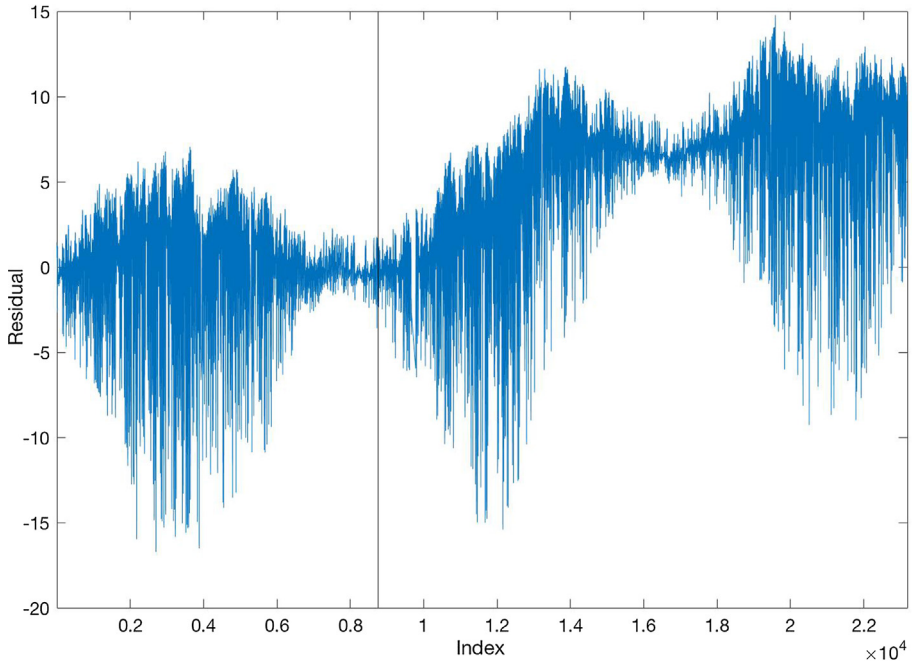

Fig. 2. Cointegrated residual series from the 8 tilt sensor signals acquired from the NPL Bridge; the vertical black line indicates the end of the training data for cointegration.

may be amplitude dependent as well. Many econometric studies have attempted to integrate seasonality into the original cointegration framework, most of them stem from [20], where seasonal unit root tests and seasonal cointegration are developed. However, this paper will look in a different direction, which is to understand the different components in the original time series, and apply cointegration on the decomposed long-term trend components. This is partly inspired by [12], which finds that cointegration tends to manifest itself on longer time scales. Thus, it can be advantageous to decompose the original time series into long-term trend components, heteroscedastic seasonality components and noise, and then apply cointegration on the trend components, which contain information that is of most interest. In the subsequent sections, the decomposition framework adopted in this paper, the TBATS model, will be reviewed in detail; the NPL Bridge will be re-examined with the proposed method in the later section.

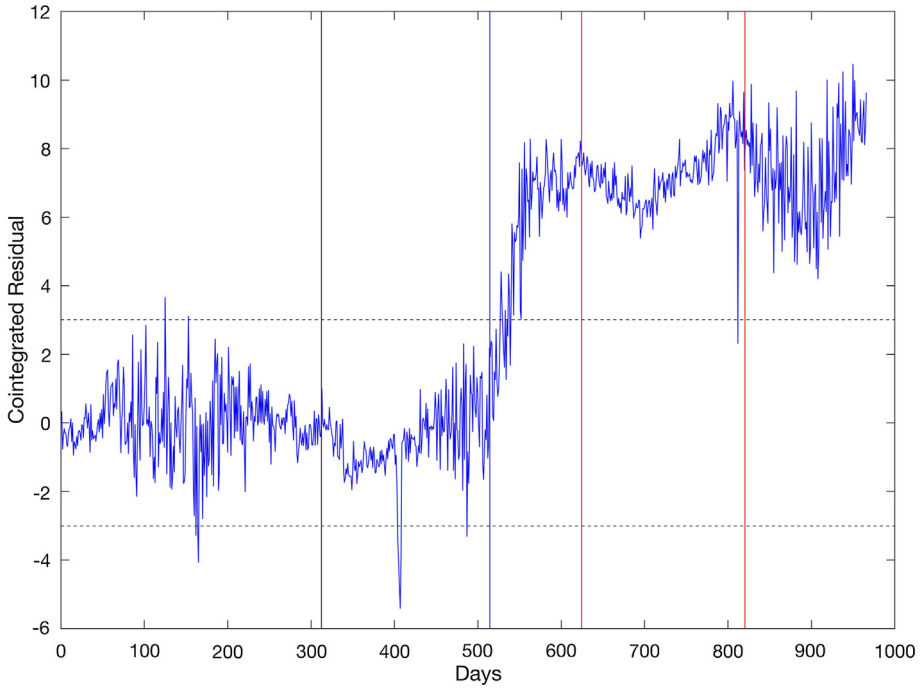

Fig. 3. X-bar chart plot of the cointegrated residual; the black vertical line indicated the end of the training data; the blue line shows when a static and dynamic test was conducted; the red lines imply damage introduction. (For interpretation of the references to colour in this figure legend, the reader is referred to the web version of this article.)

3. Exponential smoothing and TBATS model

3.1. Introduction

There are many possible solutions offered by various research communities to decompose a time series: From the perspective of signal processing, Fourier-based transforms, the discrete wavelet transform (DWT), the empirical mode decomposition, etc. are some of the mainstream methods adopted. Consider the DWT for example, it passes a raw signal through a series of quadratic mirror filters, both high-pass and low-pass filters. The high-pass filter produces details and the low-pass produces approximations. The process is repeated on the detailed signal until the last level is reached, the detail at each level expresses how the signal manifests itself at that level (scale band). In the wavelet context, each level is expressed by a number of wavelets which can be fitted to the interval of interest [12]. In the time series domain some of the classical parametric time series models have been extended in order to model nonlinear and nonstationary time series. For example, the Seasonal AutoRegressive Integrated Moving Average (SARIMA) model demonstrated in [21] attempted to accommodate the seasonality in the classical ARIMA model. Additionally, the Time-dependent AutoRegressive Moving Average (TARMA) or Time-dependent State-Space (TSS) have been developed in order to model the complex structures embedded in time series. A thorough investigation of the Functional Series TARMA (FS-TARMA) models can be found in [22]. Some literature has considered time series to be combinations of different components which exhibit distinct behaviours, examples of such components are trend components, seasonal components, and error components, and the forms of combination can be additive, multiplicative, or both [23].

Studying the characteristics of the motivating example above, this paper chooses a time series decomposition method over a signal processing method for the following reasons. First, as the magnitude of the daily cycle in the NPL data is time-varying, filter-based methods will struggle to separate this out, whereas time-series-based methods can have greater flexibility in specifying the seasonal components. Secondly, the TBATS model is selected here because it has been reported to be good at dealing with multiple seasonality in time series models, it also enables one to model multiplicative seasonal components, where other conventional time series decomposition methods, the STL decomposition for instance [24], tend to incorporate just one time-invariant seasonal component. Finally, the TBATS model is built using state space models, which enable probabilistic predictions rather than point estimates.

Exponential smoothing methods have been amongst the most widely-used and successful time series methods for decomposition and forecasting, since they were established in the late 1950s. Generally, predictions with exponential smoothing are made with weighted averages of the past observations, with the weights exponentially decaying as the observations get away from the current time instant. Recent developments have established that exponential smoothing methods

can be greatly enhanced within the framework of an innovations state space model [25]. They can not only generate the same point estimate, but also calculate the prediction intervals. The innovations state space model differs from its conventional analogue, the state space model, such that it only allows a single source of error (innovations) for both state and measurements equations, but it is more robust, and has fewer undetermined parameters; a thorough investigation on this topic can be found in [23].

3.2. TBATS model forms

Complex seasonal patterns exist in real engineering applications, for example multiple seasonality, dual-calendar effects (the coupling effect of the solar calendar and the Chinese calendar for instance [26]). To overcome this issue, De Livera et al. have introduced a novel approach based on an innovations state space model called the TBATS model [16]. The acronym 'TBATS' represents their key features: **T**rigonometric seasonality, **B**ox-Cox transformation, **A**RMA errors, **T**rend and **S**easonal components. Consider a time series $\{y_t\}_{t=1}^{N}$, the TBATS model has the following form:

$$y_t^{(\omega)} = \begin{cases} \frac{y_t^{\omega}-1}{\omega}; & \omega \neq 0 \\ \log y_t; & \omega = 0 \end{cases} \tag{1}$$

$$y_t^{(\omega)} = l_{t-1} + \phi b_{t-1} + \sum_{i=1}^{T} s_{t-1}^{(i)} + d_t \tag{2}$$

$$l_t = l_{t-1} + \phi b_{t-1} + \alpha d_t \tag{3}$$

$$b_t = (1-\phi)b + \phi b_{t-1} + \beta d_t \tag{4}$$

$$s_t^{(i)} = \sum\nolimits_{j=1}^{k_i} s_{j,t}^{(i)} \tag{5}$$

$$s_{j,t}^{(i)} = s_{j,t-1}^{(i)} \cos\lambda_j^{(i)} + s_{j,t-1}^{*(i)} \sin\lambda_j^{(i)} + \gamma_1^{(i)} d_t \tag{6}$$

$$s_{j,t}^{*(i)} = -s_{j,t-1} \sin\lambda_j^{(i)} + s_{j,t-1}^{*(i)} \cos\lambda_j^{(i)} + \gamma_2^{(i)} d_t \tag{7}$$

$$d_t = \sum\nolimits_{i=1}^{p} \varphi_i d_{t-i} + \sum_{i=1}^{q} \theta_i \epsilon_{t-i} + \varepsilon_t \tag{8}$$

Eq. (1) is the Box-Cox transformation of the series y_t, which is designed to eliminate skewness of the distribution of the data, such that the data becomes "more" normally distributed, making it easier to implement a maximum likelihood approach in the estimation part. This can be beneficial for SHM data, as this mostly tends to be non-normally distributed, although its application may also raise some concern, in light of the fact that a general SHM aim is to detect outlying data. One may choose to exclude the Box-Cox step, however, here, the idea is that damage will manifest itself by breaking the cointegration relationship, not be identified in the usual way of detected outlying points.

Eq. (2) is the main representation of the TBATS model, where $y_t^{(\omega)}$ is the transformed series of y_t, l_{t-1} is the local level at time $t-1$, and b_{t-1} is the short-run trend at time $t-1$, $s_{t-1}^{(i)}$ are the seasonal components, i is the index of the type of seasonality (as the model may allow multiple types of seasonal components), and T is the total number of types of seasonality, d_t is an ARMA process disturbance.

Eqs. (13), (4)–(8) explain the corresponding components in detail: Eq. (13) explains that the current level of the series is determined by the previous level and the short run adjustment b_{t-1} times a damping parameter ϕ; α dictates the smoothness of the level series. In Eq. (4), b is the long-run trend, b_t is the short-run trend in the period; it indicates the fact that the short-run trend consists of effects from the long-run trend and the left over short-run effect from the previous time step, the damping parameter ϕ is the same as the one in Eq. (13). In practice, the short-run adjustments can sometimes be omitted if one only wants the smooth trend series. Eqs. (5)–(7) are seasonal components based on a Fourier series with ARMA errors. Eq. (8) is a stationary ARMA residual.

3.3. Innovations state space model forms

To derive the model likelihood and subsequently estimate the model parameters, one can first rewrite the TBATS model into an innovations state space model form. For the sake of parsimony of this illustration, only two seasonal patterns are considered here, with each seasonal component consisting of only one harmonic (one frequency component); the error process is set to be an ARMA(1,1) process, i.e. $T = 2, k_1 = 1, k_2 = 1, p = 1, q = 1$. Therefore, Eq. (2) can be reorganised as:

$$y_t^{(\omega)} = l_{t-1} + \phi b_{t-1} + \sum_{i=1}^{2} s_{t-1}^{(i)} + \varphi_1 d_{t-1} + \theta_1 \epsilon_{t-1} + \varepsilon_t \tag{9}$$

The corresponding innovations state space model has the following form:

$$y_t^{(\omega)} = \mathbf{w}' \mathbf{x}_{t-1} + \varepsilon_t, \tag{10}$$

$$\mathbf{x}_t = \mathbf{F}\mathbf{x}_{t-1} + \mathbf{g}\varepsilon_t \tag{11}$$

where the state vector $\mathbf{x_t} = (l_t, b_t, \mathbf{s_t^1}, \mathbf{s_t^2}, d_t, d_{t-1}, \varepsilon_t, \varepsilon_{t-1})'$, where $\mathbf{s_t^1} = (s_{1,t}^{(1)}, s_{1,t}^{*(1)}), \mathbf{s_t^2} = (s_{1,t}^{(2)}, s_{1,t}^{*(2)})$; the emission vector $\mathbf{w}$ equals $(1, \phi, 1, 0, 1, 0, \varphi_1, \theta_1)'$, and $'$ is a transpose operator; the transition matrix $\mathbf{F}$ has the following form:

$$\mathbf{F} = \begin{bmatrix} 1 & \phi & 0 & 0 & 0 & 0 & \alpha\varphi_1 & \alpha\theta_1 \\ 0 & \phi & 0 & 0 & 0 & 0 & \beta\varphi_1 & \beta\theta_1 \\ 0 & 0 & \cos\lambda_j^{(1)} & \sin\lambda_j^{(1)} & 0 & 0 & \gamma_1^{(1)}\varphi_1 & \gamma_1^{(1)}\theta_1 \\ 0 & 0 & -\sin\lambda_j^{(1)} & \cos\lambda_j^{(1)} & 0 & 0 & \gamma_2^{(1)}\varphi_1 & \gamma_2^{(1)}\theta_2 \\ 0 & 0 & 0 & 0 & \cos\lambda_j^{(2)} & \sin\lambda_j^{(2)} & \gamma_1^{(2)}\varphi_1 & \gamma_1^{(2)}\theta_1 \\ 0 & 0 & 0 & 0 & -\sin\lambda_j^{(2)} & \cos\lambda_j^{(2)} & \gamma_2^{(2)}\varphi_1 & \gamma_2^{(2)}\theta_2 \\ 0 & 0 & 0 & 0 & 0 & 0 & \varphi_1 & \theta_1 \\ 0 & 0 & 0 & 0 & 0 & 0 & 0 & 0 \end{bmatrix}$$

and $\mathbf{g} = (\alpha, \beta, \gamma_1^{(1)}, \gamma_2^{(1)}, \gamma_1^{(2)}, \gamma_2^{(2)}, 1, 1)'$. Since TBATS models can be converted into standard innovations state space model forms, they can be nicely fitted into the framework of the Kalman filter. However, the unknown parameters, including the initial conditions, are computationally heavy to estimate, the authors in [16] used a smart algorithm to significantly reduce the computational burden, which will be briefly introduced in the following section. It is also worth noting that the above specifications are just for the simplest form of the TBATS model, one can adapt the above matrices according to specific model settings, comprehensive derivations can be found in [16].

3.4. Parameter estimation

After the Box-Cox transformation, a maximum likelihood estimation method is then used to estimate all parameters in the model. One can immediately see that the main obstacle here is the large number of parameters, which includes the damping parameter, the smoothing parameter, the Box-Cox transformation parameter, the ARMA coefficients and also the initial conditions of the innovations state space model. The trick the paper [16] employed is to make use of the single error term ε_t, and concentrate the initial conditions out of the likelihood: substituting (10) into (11), one can have $\mathbf{x}_t = \mathbf{F}\mathbf{x}_{t-1} + \mathbf{g}(y_t^{(\omega)} - \mathbf{w}'\mathbf{x}_{t-1}) = (\mathbf{F} - \mathbf{g}\mathbf{w}')\mathbf{x}_{t-1} + \mathbf{g}y_t^{(\omega)}$; then, by substituting $\mathbf{x}_t$ back to $\mathbf{x}_0$ in Eq. (13), one can have,

$$\begin{aligned} \varepsilon_t &= y_t^{(\omega)} - \mathbf{w}'\mathbf{x}_{t-1} \\ &= y_t^{(\omega)} - \mathbf{w}'\sum_{j=1}^{t-1}(\mathbf{F} - \mathbf{g}\mathbf{w})^{\mathbf{j-1}}\mathbf{g}y_{t-j}^{(\omega)} - \mathbf{w}'(\mathbf{F} - \mathbf{g}\mathbf{w}')\mathbf{x_0} \end{aligned} \tag{12}$$

From above, one can see that the initial condition $\mathbf{x_0}$ can be regarded as linearly related to the error term ε_t, therefore $\mathbf{x_0}$ can be estimated using an ordinary least squares method and substituted into the likelihood. This is one of the advantageous features of innovations state space models in comparison to the conventional state space model alternatives, it leads to savings on parameter estimation and perhaps, more accurate predictions. The representation and derivation of the likelihood is cumbersome and omitted here, readers can find the full details in [16].

3.5. Model selection

For most applications, seasonal periods are known *a priori*. In the motivating example, a daily cycle seems an obvious choice, as the measured tilts are aligned with the daily temperature cycle. Additionally, a yearly cycle is also a common seasonal period, unfortunately in the NPL data, only one year's worth of data can be used for training, making it hard to single out the yearly components from the training data. In cases where seasonal periods are unknown, one can apply a Fourier analysis on the series first to identify significant frequency components. In the scenario of multiple seasonality, one can use the Akaike Information Criteria (AIC) to evaluate every possible seasonal model, and choose the optimal model based on AIC values.

To determine the number of harmonics k_i in the seasonal components in (5), appropriate de-trending algorithms need to be applied to the original series first; then one fits the linear regression $\sum_{i=1}^{T}\sum_{j=1}^{(k_i)} a_j^{(i)}\cos(\lambda_j^{(i)}t) + b_j^{(i)}\sin(\lambda_j^{(i)}t)$ to the de-trended series. Starting from one harmonic and gradually adding more, one applies an F-test to each number of harmonics, so as to find the most significant k_i for the i^{th} seasonal component. The above procedure is repeated for every seasonal component and one computes the corresponding AIC value, increasing the number of harmonics until the minimum AIC is achieved.

To determine the orders p and q of the ARMA models, first a TBATS model without the ARMA error is fitted as a baseline model, the residual series of which will be fitted with an ARMA (p, q) model; then a model is fitted again but with an ARMA (p, q) error process. If the newly fitted model has a lower AIC value than the baseline model, the orders p and q will be accepted; otherwise, new sets of p and q will be tested, until the lowest AIC value is achieved.

3.6. Summary

TBATS can be viewed as a model decoupling the seasonality and trend components which are often modelled together in many seasonal models (SARIMA for example [21]). A few advantages that the TBATS model may offer are obvious: firstly, time varying parameters in the seasonal components (Eqs. (5)–(7) are suitable for describing changing variances in the data. Secondly, it allows for the accommodation of possible multiple seasonal effects, for example the nested effect of daily, weekly, monthly and annual periodicity, potentially suitable for analysis of operational data. Lastly, it allows any autocorrelation in the residuals to be taken into account.

However, the TBATS model can also cause trouble in a few ways: a large parameter space is set to be estimated, including the initial state of the parameter space. Furthermore, the Box-Cox transformation limits its application to only positive time series; but possible pre-processing of data can overcome this difficulty. Note that the Box-Cox transformation is an invertible transformation, one can easily recover the original series after transformation. It is also worthwhile to explore other forms of mathematical transformations, affine transformation for instance, may be a good choice [27]. Finally, irregular calendar effects might cause trouble, but this may also be addressed by introducing a dummy variable [16]. Therefore, complex seasonal variations observed in long-term monitoring data can be well modelled by the TBATS model, which can be hugely beneficial for further research.

4. Cointegration method

The concept of cointegration is based on the idea that a single time series might be difficult to accurately model and predict, but it may be more simple to find the relationship between two or more time series. To describe nonstationary time series, a common way is through the order of integration. If a time series becomes stationary after d times differencing, then this series can be said to be integrated of order d, denoted as $I(d)$. Therefore, $I(0)$ series are stationary time series, and in fact, many SHM time series are found to be $I(1)$ series. For instance, let $\{x_t\}_{t=1}^N$ and $\{y_t\}_{t=1}^N$ be two $I(1)$ time series, they are said to be cointegrated, if there exists some linear combination of them forming a stationary $I(0)$ series, explained as the following form:

$$y_t = \alpha + \beta x_t + \epsilon_t, \tag{13}$$

where ϵ_t is a stationary process. x_t and y_t each follow a nonstationary random walk process, which is unpredictable individually, but a linear combination, $y_t - \beta x_t$, becomes a stationary process which is fairly predictable. The above cointegration relationship can be easily augmented with endogenous terms such as a trend component in which the relationship is written: $y_t = \alpha + \beta x_t + \gamma t + \epsilon_t$.

Many methods have been developed to test and estimate cointegration relationships, the Engle-Granger estimation and the Johansen procedure have been perhaps the two most popular choices [28]. The former method is classically a two-stage approach; firstly the regression equation is fitted using a conventional Ordinary Least Squares (OLS) method, subsequently the residual term is tested for stationarity using the Augmented Dickey-Fuller (ADF) test. As OLS is used in the Engle-Granger method, it becomes prone to spurious regression, which means that in the scenario where in fact no cointegration exists between y_t and x_t, OLS will still produce an estimation result, which is spurious and indicates no useful information [28]. The latter approach generalises the cointegration model to the vector case, which normally starts by fitting an m-dimensional vector time series $\mathbf{X}_t$ into the following Vector Error Correction Model:

$$\Delta \mathbf{X}_t = \Pi \mathbf{X}_{t-1} + \sum_{j=1}^{p-1} \Psi_j \Delta \mathbf{X}_{t-j} + \mathbf{u}_t = AB^T \mathbf{X}_{t-1} + \sum_{j=1}^{p-1} \Psi_j \Delta \mathbf{X}_{t-j} + \mathbf{u}_t \tag{14}$$

where $\mathbf{u_t}$ is a m-dimensional vector Gaussian noise series, $\mathbf{u}_t \sim N(\mathbf{0}, \Omega)$. A and B are two $m \times r$ matrices, where r is the rank of the matrix Π. Matrix B is the cointegration vector matrix to be found, consisting of r cointegrating vectors. Matrix A is the adjustment matrix. The subsequent steps involve estimating all of the parameters with a maximum likelihood method, and performing statistical tests on the rank of the matrix B. Readers who are interested in the technical details of the Johansen procedures, may refer to [29]. In the context of SHM, cointegration is particularly useful. Loosely speaking, system variables all undergo the same sort of stochastic shifting under the influences of environmental and operational changes, even though each individual variable may be difficult to predict, the mutual relationship among them is relatively stable whenever the structure maintains intact. Or in the terms of cointegration, under normal conditions, the relevant system variables are cointegrated, the formed cointegrated residual should remain stationary as long as the health state of the structure does not change. For a full treatment of cointegration in the context of SHM, interested readers are referred to [10,30].

5. Case studies

Normally, cointegration analysis requires the noise term to be *i.i.d.* (*independent and identically distributed*) stationary Gaussian noise. In fact, an *i.i.d.* stationary Gaussian noise assumption is ubiquitous in many time series methods, which often employ ordinary least squares or maximum likelihood estimation approaches. However, *i.i.d.* stationary Gaussian noise or

homoscedastic noise is not always the case in real world applications, the existence of input dependent noise or heteroscedastic noise may therefore bias many estimation algorithms. In the context of SHM, the existence of multiple seasonality/periodicity is sometimes the source of heteroscedastic noise. Motivated by this, this paper will first separate the seasonal components from the original time series, in a attempt to suppress the associated heteroscedasticity. Cointegration is then applied to the de-seasonalised series. The proposed idea will be tested on two case studies here, a simulated cantilever beam and real monitoring data from a bridge.

5.1. Case study I: A cantilever beam

Consider a steel cantilever beam with a force applied at the free end, as shown in Fig. 4. Different thermal fields are applied to the top and bottom of the beam, so as to mimic the uneven distribution of the temperature profile of a structure operating in a real environment. In addition, to mimic the daily and seasonal patterns, and a linear trend of temperature in the real world, the temperature fields T_1 and T_2 are imposed to be:

$$T_1 = 10 \times \left\{ \sin(12\pi t) + \sin(4\pi t) + 3t \times 10^{-3} - 2 \right\}$$
$$T_2 = 8 \times \left\{ \sin(12\pi t - 0.5\pi) + \sin(4\pi t) + 3t \times 10^{-3} - 2 \right\}$$

As the beam is simulated as an isotropic material, the temperature of the beam monotonically decreases from the top to the bottom, with a linear gradient, which is illustrated in the cross-sectional plot in Fig. 4. 10000 sample points are simulated, as

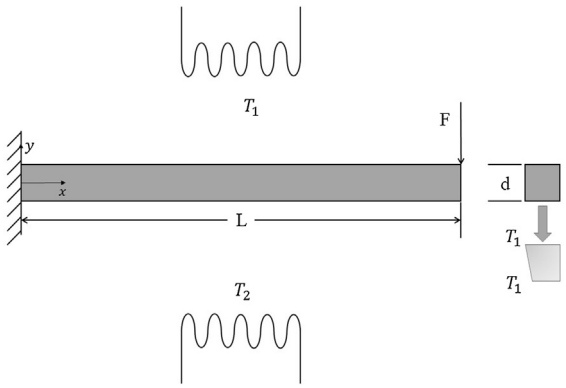

Fig. 4. Schematic plot of a cantilever beam with a force applied at the end; the top and bottom of the beam are applied with different temperature fields, the cross-section plot shows the gradient distribution of temperature.

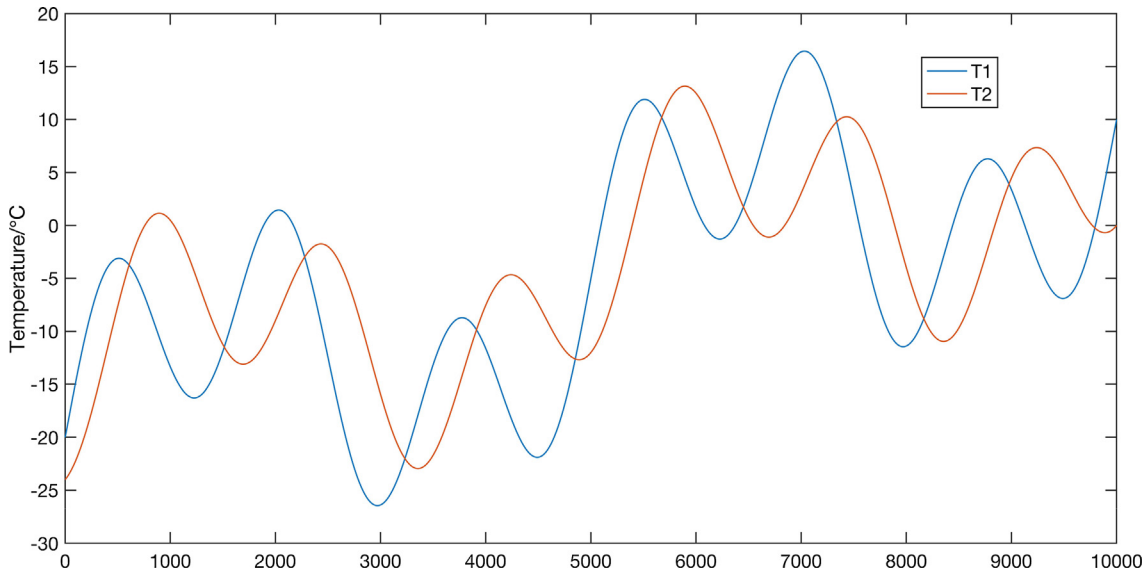

Fig. 5. Temperature of the top of the cantilever beam T_1, and temperature of the bottom T_2.

shown in Fig. 5. Because temperature is assumed to change over time, the stress and deflection of the beam will also change accordingly. There are two reasons why the beam's deflection will change with temperature; firstly, the Young's modulus of steel is normally considered to be linearly correlated with temperature; secondly, the temperature gradient of the beam will also change with time, thus the thermal expansion of the beam will be varying with time. The angle of rotation of the beam is therefore composed of two parts, mechanical and thermal rotation, as expressed in the following equations:

$$\begin{aligned} Thermal: \theta_T &= \frac{\alpha(T_1 - T_2)x}{d} \\ Mechanical: \theta_M &= \frac{F(-Lx + \frac{1}{2}x^2)}{EI} \\ Overall: \theta &= \theta_T + \theta_M \end{aligned}$$

where α is the thermal expansion coefficient, and x is the position of the beam from the fixed-point at the left end.

5.1.1. Simulations

The thermal field in Fig. 5 is applied to the cantilever beam and the angles of rotation of four positions on the beam, $(0.25L, 0.5L, 0.75L, L)$, are evaluated. 4×10000 samples points are therefore obtained. It is not uncommon in engineering that measurement noise can be input-dependent, or in econometric terms, heteroscedastic noise. To simulate this situation, an amplitude-dependent Gaussian noise is added to the theoretical results, as expressed by the following:

$$\hat{\theta} = \theta + 0.1 \times \theta \times \epsilon_t$$

where $\hat{\theta}$ is the measured rotation, and ϵ_t is Gaussian noise with $\epsilon_t \sim N(0, 1)$. The measurements with heteroscedastic noise corruption are plotted in Fig. 6.

To simulate damage, the stiffness of the beam is reduced by 50% after data point 7500, as illustrated by a black vertical line in Fig. 6. Although damage is introduced, only a slight shift in amplitude is visible; changes due to temperature variations are still dominant.

5.1.2. Results

If one uses the conventional cointegration method to cointegrate the four series with the training set ranging from point 1 to 5000, the cointegrated residual series is shown in Fig. 7. As expected, the heteroscedastic noise sabotages the required condition of normally-distributed noise, which comes from the fact that the Johansen procedure is a maximum likelihood method.

The TBATS decomposition is therefore applied, in order to extract the daily and seasonal components first, before application of the cointegration method. A representative result of the decomposition of X_1 is shown in Fig. 8. One can see that the seasonal and daily patterns have been accurately identified and that most of the noise is left in the level term. Damage information can also be clearly discerned in the level term.

Although damage information is clear in this case, it is likely that in other scenarios, the trend term itself is great enough to disguise the damage information. The de-seasonalised series are subsequently fed to cointegration and the cointegrated residual series is now shown in Fig. 9. With the three standard deviation confidence interval overlaid, the plot is much clearer than Fig. 7, the residual stays mostly stationary in the mean and the nonstationary level in the variance has also been somewhat suppressed; most importantly the damage information is evident immediately after it is introduced.

5.2. Case study II: The NPL bridge

Continuing with the motivating example of the NPL Bridge in Section 2, this section will present more details of the SHM of the NPL Bridge, and revisit the heteroscedastic issue concerned with the NPL Bridge, the subsequently attempt to address it with the proposed method.

5.2.1. The SHM of the NPL bridge

The NPL Bridge is 20 m long and 5 m high, weighing around 15 tonnes, as illustrated in Figs. 10 and 11. After it was in service for nearly 50 years, the bridge was moved to a new location to conduct long-term monitoring experiments with a variety of different sensors, during the years 2009 to 2011. The monitoring covered an extensive time period consisting of at least two full seasonal variations. The monitoring campaign implemented several testing events, the respective time lines are summarised in Fig. 12. The bridge was subjected to a series of static short-term and sustained loading tests, starting from March 2009. Loading was employed with water tanks of different weights, at the edge of the bridge deck, as illustrated in the left end of Fig. 10. Apart from loading tests, a few damage scenarios were also realised on the bridge; on 18th October 2010 for example, artificial damage was introduced by cutting the rebar on the top of the bridge deck, so as to represent the decrease of the cross section. A number of other test events were also implemented, readers can find details from [31].

As mentioned above, this bridge was heavily instrumented with many kinds of sensors, but only the tilt sensor data will be analysed in this study. The tilt sensors were installed by the ITMSOIL instrumental company in December 2008; Fig. 10 shows the schematic of all the locations of the 8 tilt sensors. Tilt sensors are used to measure the local inclination of the

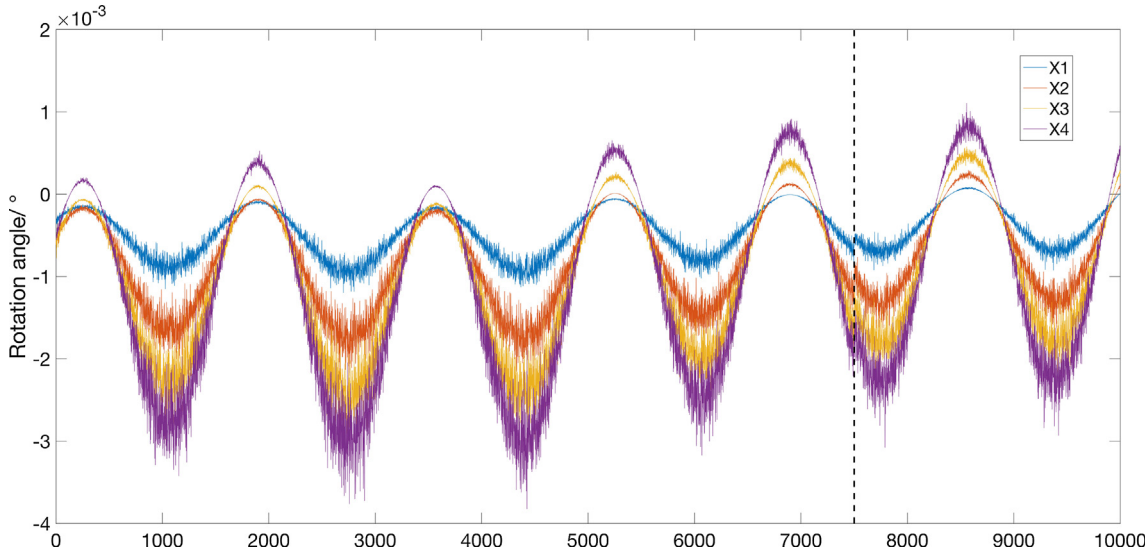

Fig. 6. The angles of rotation measured at the four positions $(0.25L, 0.5L, 0.75L, L)$ of the beam, corrupted with heteroscedastic noise; the black vertical line indicates where damage is simulated.

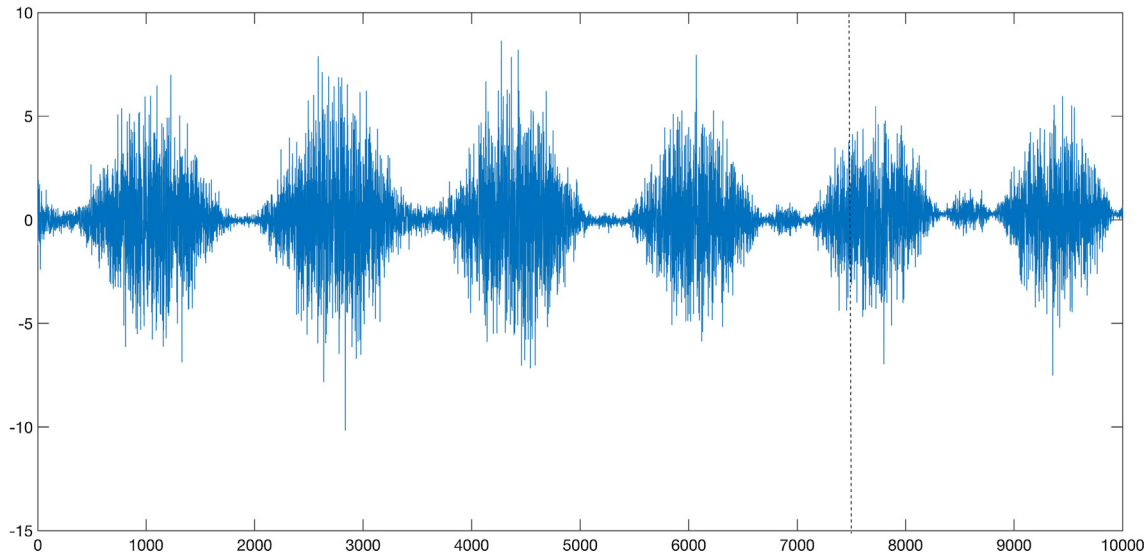

Fig. 7. The residual series obtained using the conventional cointegration method, the vertical dashed line marks where damage is introduced.

structure, therefore they can potentially be used to indicate the onset of damage in the structure. The data were originally collected at a five-minute time interval except for a number of days of special tests. Consequently, before doing any analysis, the first thing is to make the data regularly sampled. As the data were carefully labelled with a time stamp, the data on the hour were used to form a new time series, a representative example of the tilt sensor 1 (TL1) data is shown in Fig. 12, the time stamps for the important test events are summarised in Table 1.

Notice that in the original study of the monitoring campaign, thermal sensors were also installed on multiple positions of the bridge. However, after investigating the origins of measurement uncertainty, Barton and Esward [17] found that the temperature measurements at different locations of the bridge might have a lagged effect due to the temperature gradients caused by heating from the sun. In this study, temperature data will not be used, as cointegration is able to remove environmental variations without the measurements of the environmental variables.

5.2.2. Results and discussion

It is not difficult to see from Fig. 12 that the tilt sensor measurements are quite nonstationary, both in mean and variance. The changes in mean could be caused by environmental variations or destructive test implementation, and obviously any

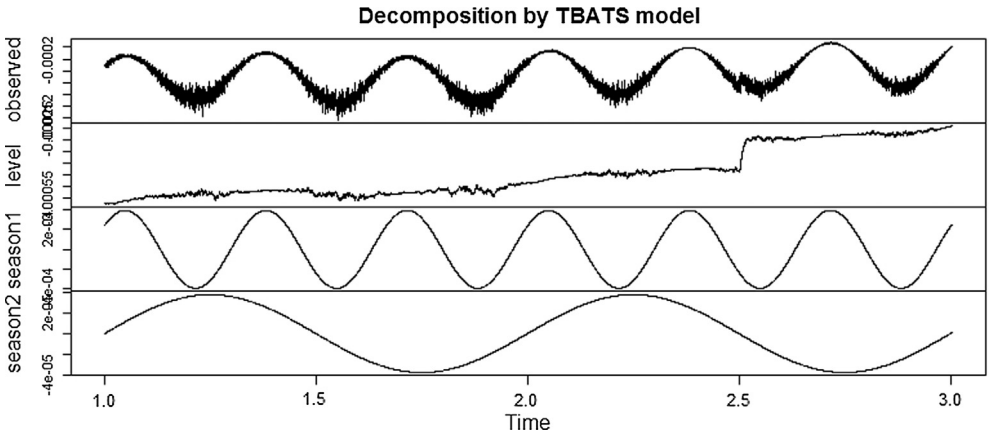

Fig. 8. Decomposition results from the TBATS model: the first row is the original time series, the second row is the decomposed level series, the third row and the fourth row represent the two different seasonal components.

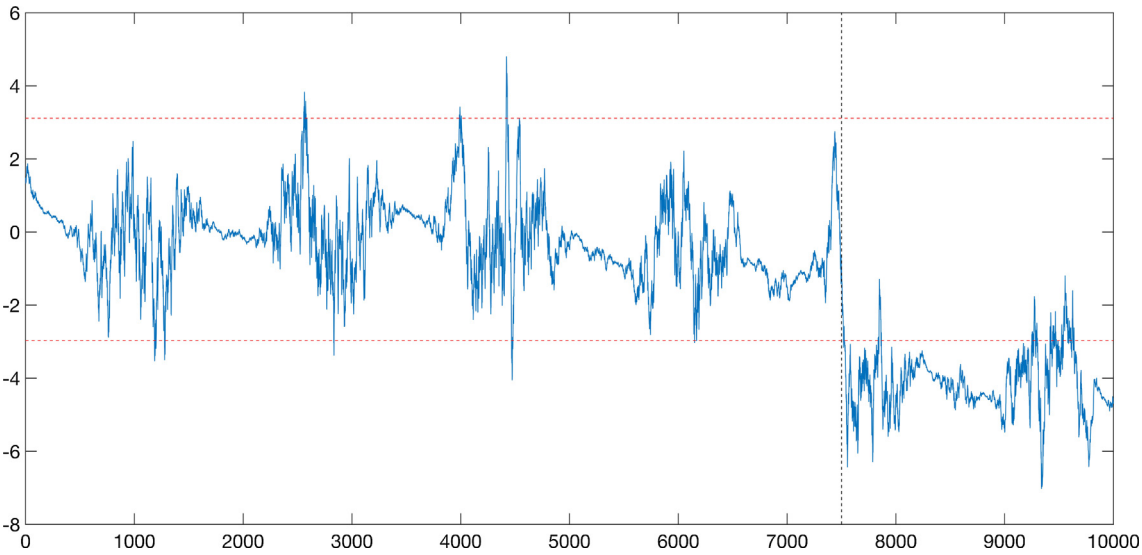

Fig. 9. Cointegrated residual series of the de-seasonalised series; red horizontal lines indicate three standard deviation intervals; black vertical line marks the damage introduction point. (For interpretation of the references to colour in this figure legend, the reader is referred to the web version of this article.)

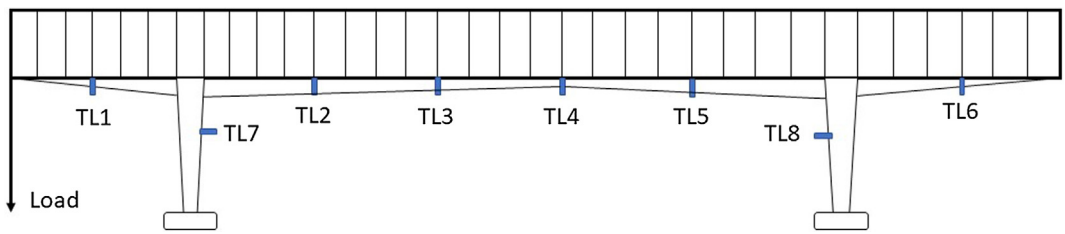

Fig. 10. Layout of all tilt sensors on the bridge and the loading implementation position.

potential changes induced by damage are overwhelmingly masked by environmental variations. While the changes in the variance are a bit more complex, one can roughly observe that the volatility level in the winter time is significantly smaller than that in the summer time, and the volatility level has a repeated pattern resembling seasonal variations. As the measurements were taken over a time period of two years and eight months, two complete seasonal cycles can be visualised; the first ranges from February 2009 to February 2010, the second seasonal cycle starts in February 2010 and ends in February 2011.

Fig. 11. The photo of the NPL Bridge in situ.

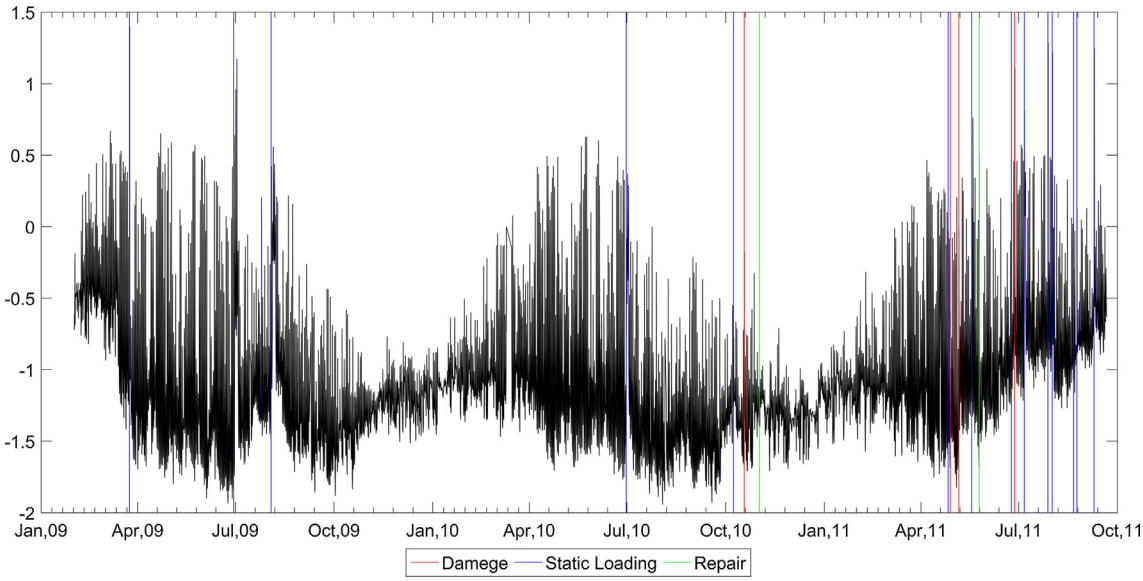

Fig. 12. Timetable of the respective destructive tests implemented on the NPL Bridge and hourly data of tilt sensor 1 (TL1) during February 2009 to September 2011.

Table 1
Important test events and their corresponding time stamps.

Index	Time	Test Event
1	2009.03.24	Static loading
2	2009.06.29	Static loading
3	2009.08.03	Static loading
4	2010.06.30	Static/Dynamic loading
5	2010.10.08	Static loading
6	2010.10.18	Damage: removing the rebar
7	2010.11.01	Repairing damage

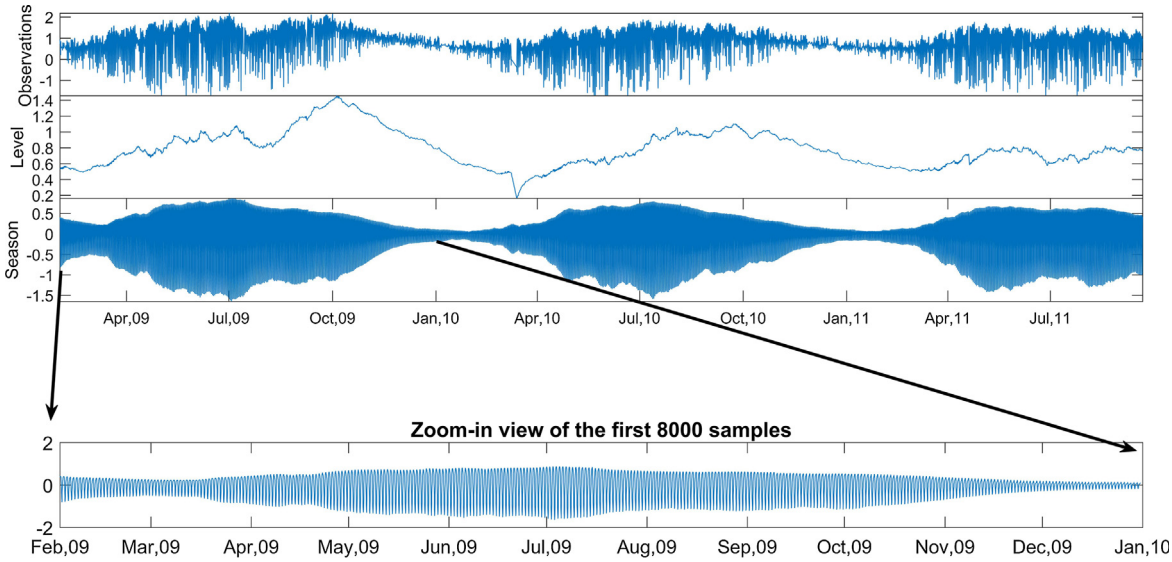

Fig. 13. A single seasonal TBATS decomposition of the tilt sensor 6 (TL6) data: the first row is the original time series, the second row is the decomposed level series, the third row shows the decomposed seasonal series, and the plot below shows the zoom-in view of the first 8000 samples of the decomposed seasonal series.

Barton and Esward found that the thermal expansion of this bridge was unexpectedly large and complex, it could produce almost the same strain level that was caused by a two-tonne loading [17].

As mentioned above, cointegration has been developed to deal with environmental and operational variations and the Johansen procedure is normally used to estimate cointegration relationships. However, the Johansen procedure is a likelihood-based method, which would naturally require the residuals to be an *i.i.d.* process; marked seasonality in the data would therefore sabotage this condition and underestimate the variance level. In this paper, the TBATS time series decomposition method will be employed first, in order to concentrate out the underlying complex seasonal components; subsequently, a normal cointegration analysis will be carried out to the de-seasonalised series.

A representative example of the TBATS decomposition of the sixth tilt sensor data is shown in Fig. 13. The top plot is the original time series, the decomposed components are shown in the middle and bottom plots, and they are the level and seasonal series respectively. The level series can be thought to be the extracted trend of the original series, purged of observation noise and seasonality. One can see that the level series is much smoother than the original series, most of the fluctuations have been removed, and the long-term trend is well preserved. The seasonal pattern is set to be 24 h (daily cycle), as expressed in Eqs. (5)–(7), which means that the seasonal series has a daily pattern whose magnitude changes over time. Comparing the shape of the envelope of the seasonal series with the original series, most of the time-varying daily cyclic components have been accurately singled out, potential damage information is manifested in the long-run component, the trend component, hence cointegration can be subsequently applied for damage detection.

After conducting TBATS decompositions to each of the eight tilt sensor datasets, one can obtain eight de-seasonalised trend series and error series. The data ranging from February 2009 to February 2010 are used to form a training set, as this period covers a full seasonal variation. The Johansen procedure is then applied to the eight trend component series using the training data set, in order to estimate a cointegration relationship. A residual series is then formed using the whole data set, as shown in Fig. 14. The shaded area in the figure indicates a 95% confidence interval. The region between the beginning of the series and the first black vertical line consists of the training set. Apart from a few occurrences of alarms, the series stays mostly stationary, and the changes caused by environmental variations are largely eliminated. The blue vertical line at

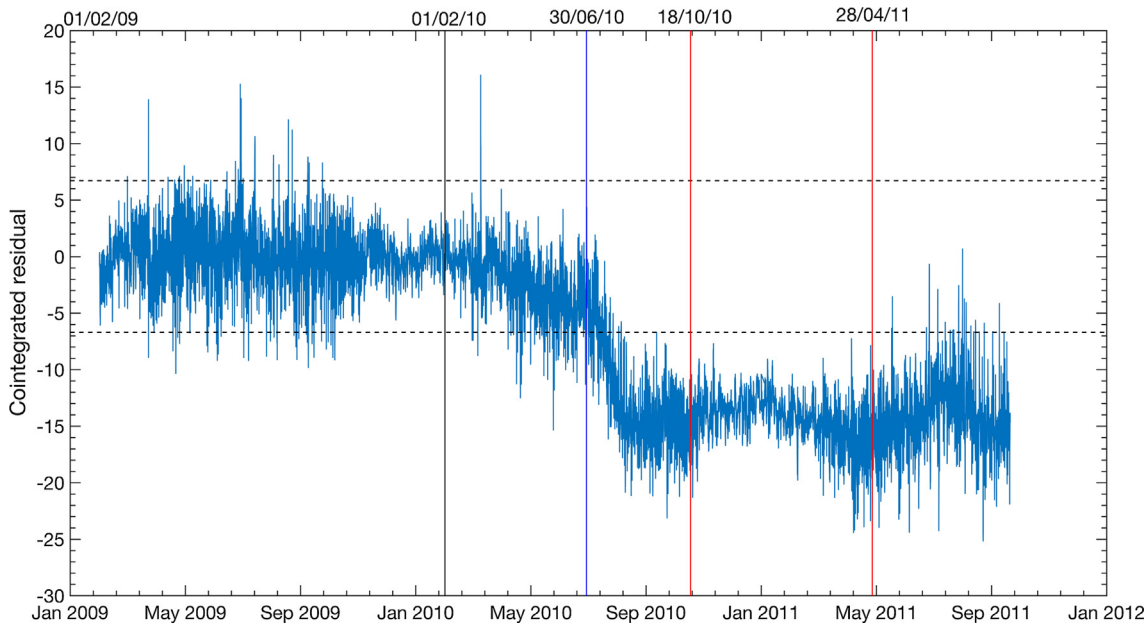

Fig. 14. Cointegrated residual with confidence intervals marked with black horizontal lines; the black vertical line indicated the end of the training data; the blue line shows when a static and dynamic test was conducted; the red lines imply damage introduction. (For interpretation of the references to colour in this figure legend, the reader is referred to the web version of this article.)

around June 30th 2010 indicates when a major static test was conducted. One can see that after this date, the residual series has a major shift in the mean and also exceeded the lower confidence boundary, which can be regarded as a clear alarm signal. This can be explained by the fact that once the health state of the structure has changed, the underlying cointegration relationship may no longer hold, and consequently the cointegrated residual will no longer stay stationary.

From Fig. 12, it is also known that after June 30th, the campaign implemented a few other events on this bridge. It is worth noticing that on May 6th 2011, the campaign introduced a severe damage (removing the damaged concrete) to the bridge. Correspondingly on Fig. 14, the mean level of the residual series undergoes a significant increase after this date, which is an indication that the bridge is experiencing a change of state. Although the mean of the residual seems to return to the mean of the training set, it certainly does not mean that the bridge is recovering to its healthy state. In order to further detect any damage after June 30th, one would possibly need to re-evaluate the latest cointegration relationship of the bridge, and form a new state of "normal condition'.

5.2.3. Comparison with the linear cointegration method

Comparing the results in Fig. 14 with the cointegrated residual plotted in Fig. 3, one can draw the following conclusions:

First of all, the heteroscedastic noise in the residual has been significantly suppressed, the residual series before the first blue line is quite stationary both in mean and variance, the environmental variations have been largely purged; this confirms the assumption that most of the heteroscedasticity is manifested in the seasonal components;

Secondly, Fig. 14 has accurately captured the long-term trend component; any information about structural changes to the bridge is well reflected in the residual series. For example, on June 30th 2010, the monitoring campaign conducted both static loading and dynamic loading on the bridge, the residual in the figure presents a sudden drop in the mean and exceeds the lower confidence interval soon after the time mark. It was observed that early cracking had been developed in the bridge weeks after the test on March 24*th*, 2009; static and dynamic tests further deteriorated the condition of the bridge, thus one can observe a gradual development of damage in the residual series [18]. In contrast, in Fig. 2, the underlying trend is overwhelmed by the heteroscedastic noise. Interestingly, the residual series behaves quite differently even after it goes beyond the control limit; for example, points between the two red lines and the points after the second red line show distinct characteristics. However, one needs to notice that once the cointegration relationship has 'broken", it is necessary to update with a new cointegration relationship, and a new cointegrated residual needs to be estimated as well.

The TBATS model above has successfully dealt with heteroscedastic noise, but if one also wishes to apply the X-bar chart, similar to the one used in [18], it is trivial to obtain the plot, shown in Fig. 15. Comparing with Fig. 12, one obvious improvement is that the time varying variance has been eliminated here, the residual during the undamaged condition maintains stationary. Although, near the first blue line, the residual gives early alarms, this is probably because that the TBATS model is an off-line method in nature, meaning that it has to decompose the series as a whole, which may smooth out sharp changes in the trend component.

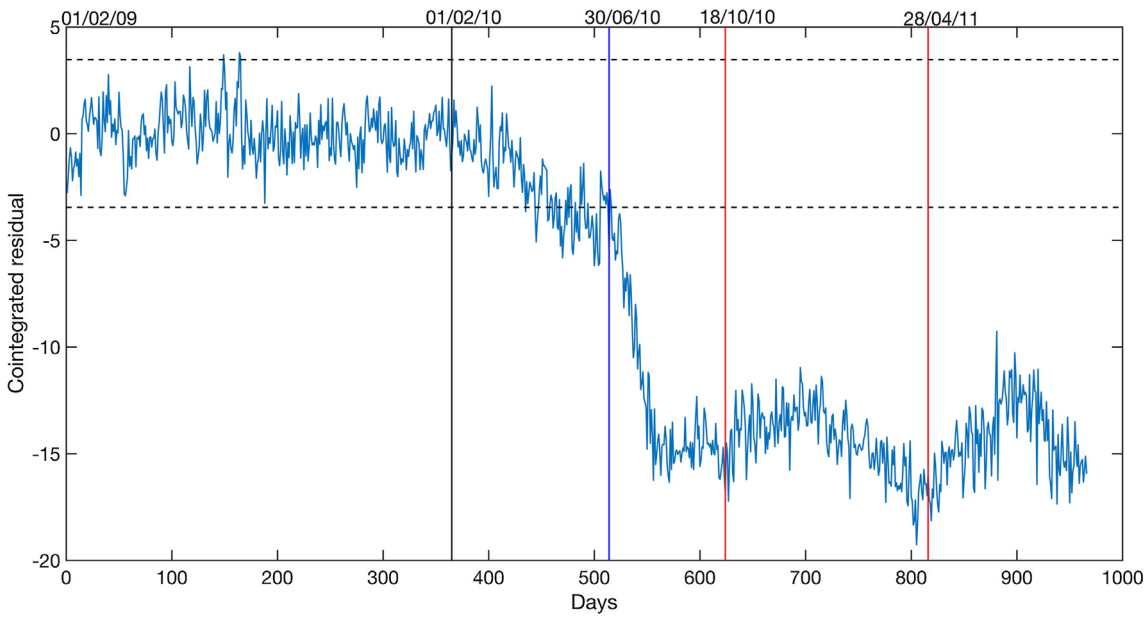

Fig. 15. X-bar chart for the cointegrated residual; the black vertical line indicates the end of the training data; the blue line shows when a static and dynamic test was conducted; the red lines imply damage introduction. (For interpretation of the references to colour in this figure legend, the reader is referred to the web version of this article.)

Moreover, from a practical perspective, if one wishes to apply the proposed algorithm to a real world engineering practice, say the SHM of a bridge in operation, one would first need to acquire sufficient amount of sensor measurements of the bridge under healthy conditions; then, the proposed method can be used to build a baseline model and a baseline residual series; as new data come in, the TBATS decomposition is applied on the whole dataset, including training data and newly-arrived data, followed by the cointegration analysis; finally, the baseline model can be updated on a regular basis, in order to improve computational efficiency.

6. Conclusions

In this paper, an extension of previous studies of the cointegration method for SHM has been explored. The TBATS model from the time series community has been tested in order to project out the seasonality observed in SHM data. The TBATS model is a flexible and robust state space model with a single source of error, which has been widely adopted in the analysis of seasonal time series. As long-term SHM data are inevitably affected by daily, seasonal and annual environmental variations, and maybe in some cases the interactions of human activities, it will be beneficial if the seasonal component can be extracted before doing subsequent analysis. As cointegration has proved to be a powerful tool to deal with the issue of environmental and operational variations in SHM, the TBATS model can be seen as a pre-processing tool for cointegration analysis. By removing the seasonality one may potentially suppress the heteroscedastic noise caused by it, and as the Johansen procedure for cointegration would normally require the noise to be an *i.i.d.* process, this might help to rectify any ill-conditioned procedures. In the fourth section of the paper, two case studies were presented. A synthetic case simulates a cantilever beam under varying temperature conditions; heteroscedastic noise is added to the simulations. The TBATS model is first used to separate the two seasonal components and then the cointegration approach is applied, damage information can then be visualised in the residual series. Another case study of the NPL bridge is presented with the proposed method. The result is encouraging, in that the TBATS model can elegantly extract the daily cycles from the original series and most of the heteroscedasticity is accounted for by the seasonal components. The long term trend series is then used in a cointegration analysis, the resulting residual series is mostly stationary in the training set, with most of the environmental variations removed, the residual series remains sensitive to damage information.

Acknowledgements

The work is funded by the China Scholarship Council (Grant No. 201406830013) and the support of the UK Engineering and Physical Sciences Research Council (EPSRC) through grant reference numbers EP/J016942/1 and EP/K003836/2 is gratefully acknowledged. The authors also thank Dr. Elena Barton from the National Physical Laboratory for providing us with the data of the NPL bridge project.

References

[1] C.R. Farrar, K. Worden, Structural Health Monitoring: A Machine Learning Perspective, John Wiley & Sons, 2012.
[2] J. Ko, Y. Ni, Technology developments in structural health monitoring of large-scale bridges, Eng. Struct. 27 (12) (2005) 1715–1725.
[3] S. Soyoz, M.Q. Feng, Long-term monitoring and identification of bridge structural parameters, Comput.-Aid. Civ. Infrastruct. Eng. 24 (2) (2009) 82–92.
[4] C.-Y. Kim, D.-S. Jung, N.-S. Kim, S.-D. Kwon, M.Q. Feng, Effect of vehicle weight on natural frequencies of bridges measured from traffic-induced vibration, Earthquake Eng. Eng. Vib. 2 (1) (2003) 109–115.
[5] H. Sohn, Effects of environmental and operational variability on structural health monitoring, Philos. Trans. R. Soc. London A: Math. Phys. Eng. Sci. 365 (1851) (2007) 539–560.
[6] E. Reynders, G. Wursten, G. De Roeck, Output-only structural health monitoring in changing environmental conditions by means of nonlinear system identification, Struct. Health Monit. 13 (1) (2014) 82–93.
[7] L.D. Avendaño-Valencia, E.N. Chatzi, K.Y. Koo, J.M. Brownjohn, Gaussian process time-series models for structures under operational variability, Front. Built Environ. 3 (2017) 69.
[8] K. Worden, E. Cross, On switching response surface models, with applications to the structural health monitoring of bridges, Mech. Syst. Sig. Process. 98 (2018) 139–156.
[9] J. Kullaa, Distinguishing between sensor fault, structural damage, and environmental or operational effects in structural health monitoring, Mech. Syst. Sig. Process. 25 (8) (2011) 2976–2989.
[10] E.J. Cross, K. Worden, Q. Chen, Cointegration: a novel approach for the removal of environmental trends in structural health monitoring data, Proc. R. Soc. London A: Math. Phys. Eng. Sci. 467 (2011) 2712–2732, The Royal Society.
[11] G. Vidyamurthy, Pairs Trading: Quantitative Methods and Analysis, Vol. 217, John Wiley & Sons, 2004.
[12] K. Worden, E. Cross, I. Antoniadou, A. Kyprianou, A multiresolution approach to cointegration for enhanced SHM of structures under varying conditions–an exploratory study, Mech. Syst. Sig. Process. 47 (1) (2014) 243–262.
[13] H. Shi, K. Worden, E. Cross, A nonlinear cointegration approach with applications to structural health monitoring, in: Journal of Physics: Conference Series, Vol. 744, IOP Publishing, 2016, p. 012025.
[14] K. Zolna, P.B. Dao, W.J. Staszewski, T. Barszcz, Towards homoscedastic nonlinear cointegration for structural health monitoring, Mech. Syst. Sig. Process. 75 (2016) 94–108.
[15] K. Worden, T. Baldacchino, J. Rowson, E.J. Cross, Some recent developments in SHM based on nonstationary time series analysis, Proc. IEEE 104 (8) (2016) 1589–1603.
[16] A.M. De Livera, R.J. Hyndman, R.D. Snyder, Forecasting time series with complex seasonal patterns using exponential smoothing, J. Am. Stat. Assoc. 106 (496) (2011) 1513–1527.
[17] E. Barton, T. Esward, The origins of measurement uncertainty in SHM-NPL footbridge case study, 6th European Workshop on Structural Health Monitoring, 2012.
[18] K. Worden, E. Cross, E. Barton, Damage detection on the npl footbridge under changing environmental conditions, 6th European Workshop on Structural Health Monitoring, 2012, pp. 1–8.
[19] D.C. Montgomery, Introduction to Statistical Quality Control, John Wiley & Sons, New York, 2009.
[20] S. Hylleberg, R.F. Engle, C.W. Granger, B.S. Yoo, Seasonal integration and cointegration, J. Econom. 44 (1–2) (1990) 215–238.
[21] P. Omenzetter, J.M.W. Brownjohn, Application of time series analysis for bridge monitoring, Smart Mater. Struct. 15 (1) (2006) 129.
[22] M. Spiridonakos, S. Fassois, Non-stationary random vibration modelling and analysis via functional series time-dependent arma (fs-tarma) models–a critical survey, Mech. Syst. Sig. Process. 47 (1–2) (2014) 175–224.
[23] R. Hyndman, A.B. Koehler, J.K. Ord, R.D. Snyder, Forecasting with Exponential Smoothing: The State Space Approach, Springer Science & Business Media, 2008.
[24] R.B. Cleveland, W.S. Cleveland, I. Terpenning, Stl: A seasonal-trend decomposition procedure based on loess, J. Off. Stat. 6 (1) (1990) 3.
[25] C.C. Holt, Forecasting seasonals and trends by exponentially weighted moving averages, Int. J. Forecast. 20 (1) (2004) 5–10.
[26] H.-L. Lin, L.-M. Liu, Y.-H. Tseng, Y.-W. Su, Taiwan's international tourism: a time series analysis with calendar effects and joint outlier adjustments, Int. J. Tour. Res. 13 (1) (2011) 1–16.
[27] C.W. Granger, J. Hallman, Nonlinear transformations of integrated time series, J. Time Ser. Anal. 12 (3) (1991) 207–224.
[28] W. Enders, Applied econometric time series, Technometrics 46 (2) (2004) 264.
[29] S. Johansen, Likelihood-based Inference in Cointegrated Vector Autoregressive Models, Oxford University Press, 1995.
[30] E. Cross, On Structural Health Monitoring in Changing Environmental and Operational Conditions Ph.D. thesis, University of Sheffield, 2012.
[31] V. Livina, E. Barton, A. Forbes, Tipping point analysis of the NPL footbridge, J. Civ. Struct. Health Monit. 4 (2) (2014) 91–98.